SAR COMPLIANCE TESTING OF CISCO MODEL AIR-CB20A-A-K9 (FCC ID# LDK102044)

PC CARD INSERTED INTO A LAPTOP COMPUTER

May 29, 2002

Submitted to:

Mr. Jim Nicholson
EMC Compliance Engineer
EAG WNBU Engineering
Cisco Systems, Inc.
320 Springside Drive, Suite 350
Akron, Ohio 44333

Submitted by:

Om P. Gandhi
Professor of Electrical and Computer Engineering
University of Utah
50 S Central Campus Dr., Rm. 3280
Salt Lake City, UT 84112-9206

SAR COMPLIANCE TESTING OF CISCO MODEL AIR-CB20A-A-K9 (FCC ID# LDK102044) PC CARD INSERTED INTO A LAPTOP COMPUTER

I. Introduction

The U.S. Federal Communications Commission (FCC) has adopted limits of human exposure to RF emissions from mobile and portable devices that are regulated by the FCC [1]. The FCC has also issued Supplement C (Edition 97-01) to OET Bulletin 65 [2] and a more recent version of the same [3] defining both the measurement and the computational procedures that should be followed for evaluating compliance of mobile and portable devices with FCC limits for human exposure to radiofrequency emissions.

We have used both the measurement and computational procedures for SAR compliance testing of the Cisco Model PC Card (FCC ID# LDK102044) inserted into a Laptop computer. A photograph of the unit with the Cisco Model AIR-CB20A-A-K9 PC Card inserted into a laptop computer is given in Fig. 1. A picture of the Model AIR-CB20A-A-K9 PC Card placed on the laptop is given in Fig. 2. The Cisco Model AIR-CB20A-A-K9 PC Card operates over the frequency band 5150 to 5350 MHz with a nominal transmit power of 13.2 dBm (20.9 mW).

An engineering drawing of the Model AIR-CB20A-A-K9 PC Card is given in Fig. 3. For spatial diversity, the Model AIR-CB20A-A-K9 PC Card uses two rectangular patch antennas each of dimension 0.67" × 0.61". Also used for each of the antennas is a parallel rectangular parasitic patch of identical dimensions 0.67" × 0.61" with a separation of 0.79" above the driven elements. At any given time, one of the two antennas is used as a transmitting antenna while the other is used as a receiving antenna.

For SAR measurements, two configurations of the wireless PC relative to the experimental phantom have been used:

a. Since the wireless PC may possibly be placed on a user's lap where the RF antennas would be the closest to the body, a planar phantom model with inside dimensions 12" × 16.5" (30.5 × 41.9 cm) and a base thickness of 2.0 ± 0.2 mm (recommended in [3]) was used

for SAR measurements and the wireless PC cards mounted in a portable computer (as in Fig. 1) pressed against the bottom of this phantom (see Fig. 4).

b. For a bystander, the "end-on" SAR value is obtained for the PC and the card edge at 90° to the flat phantom with a spacing of 2.5 cm (see Fig. 5).

II. Computation of SAR Distributions

The Finite Difference Time-Domain Method

One of the most successful and versatile methods for SAR calculations is the finite-difference time-domain (FDTD) method. This method was first proposed by Yee [4] and later developed by Taflove and colleagues [5-7], Holland [8], and Kunz and Lee [9]. This method has been extensively used for calculations of the distributions of electromagnetic (EM) fields and SARs in anatomically-based models of the human body for whole-body or partial-body exposures due to far-field or near-field irradiation conditions [10, 11]. In this method, the time-dependent Maxwell's curl equations

$$\nabla \times \mathbf{E} = -\mu \frac{\partial \mathbf{H}}{\partial t}, \qquad \nabla \times \mathbf{H} = \sigma \mathbf{E} + \varepsilon \frac{\partial \mathbf{E}}{\partial t} \tag{1}$$

are implemented for a lattice of subvolumes or "cells" that may be cubical or parallelepiped with different dimensions δ_x, δ_y, and δ_z in x-, y-, or z-directions, respectively. The components of **E** and **H** are positioned about each of the cells as shown in Fig. 6 and calculated alternately with half-time steps where the time step $\delta t = \delta/2c$ where δ is the smallest of the dimensions used for each of the cells and c is the maximum phase velocity of the fields in the modeled space. Since some of the modeled volume is air, c corresponds to the velocity of EM waves in air. The details of the method are given in several of the above referenced publications [4-9] and will, therefore, not be repeated here.

In the FDTD method, it is necessary to represent not only the absorber/scatterer such as the human body or a part thereof, but also any near-field source/s such as the two antenna and the rest

of the circuit given in Fig. 3. Since the SAR distribution is critically dependent on the antenna geometry and its placement vis à vis the lossy planar model simulant of the human lap, this region was modeled with an FDTD cell size of 0.4 × 0.4 × 0.4 mm. This choice of the FDTD cell dimension allowed a proper representation of the four patches of the two antennas, each of dimension 0.67" × 0.61" (17.02 × 15.49 mm) by 42 × 39 cells. Similarly, the entire PC board of Fig. 3(c) of width 1.7827" (45.28 mm) was modeled by 113 cells and its length was modeled by 120 cells (48 mm or 1.89"). The highest SAR region is immediately under the edge of the PC board for the transmitting antenna, and this region is modeled quite appropriately. For the Cisco Model AIR-CB20A-A-K9 PC Card, each of the antennas is fed by a microstripline of width 0.0634" (1.61 mm) which was modeled by four FDTD cells each of width 0.4 mm. Similarly, there are two notches one on either side of the microstrip feed lines each of width 0.0631" (1.60 mm) and these were also modeled with four FDTD cells each of width 0.4 mm. The dielectric constant of the material between the two driven patches and the parasitic patches and also for the substrate of the printed antenna was assumed to be 2.2 (Duroid). The spacing between the driven and the parasitic patches of 0.079" (2.0 mm) was modeled by five FDTD cells and the spacing between the driven patches (and the microstrip feed line) and the ground plane underneath of 0.032" (0.81 mm) was modeled by two cells.

For SAR calculations, we have assumed a planar tissue-simulant lossy phantom at a distance of 1 cm (modeled by 25 cells) below the ground plane of the PC board. Even though the experimental planar phantom is of internal dimensions 12" × 16.5" (30.5 × 41.9 cm) and base thickness 2 mm, only a limited volume of this is modeled for SAR calculations. This is justified since the electromagnetic fields of the PC card are highly localized to the region in close proximity to the antenna and the volume underneath. Because of the use of the PML boundary condition for the FDTD, it is possible to truncate the problem without encountering artefactual reflections [12]. For the present problem, we have taken a problem space grid of 150 × 160 × 180 or 4.32 million cells. For the tissue-simulant lossy medium, we have used the dielectric properties $\varepsilon_r = 48.9$ and $\sigma = 5.42$ S/m extrapolated from the dielectric properties recommended at 3.0 and 5.8 GHz in [3].

For a conducted power of 13.2 dBm (20.9 mW), the calculated peak 1-g SAR for the Cisco Model AIR-CB20A-A-K9 PC Card at the midband irradiation frequency of 5.25 GHz is 0.146 W/kg for a planar phantom with 2 mm base thickness (acrylic polystyrene with $\varepsilon_r = 2.56$). Though not measured, the loss tangent given for acrylic polystyrene in the ITT Handbook is 0.00033 at 3 GHz and 0.0012 at 25 GHz [13]. Thus the loss tangent is considerably lower than 0.05 suggested as the upper limit in FCC Supplement C ed. 01-01 [3]. As expected, the peak 1-g SAR was lower and only 0.106 W/kg if a base thickness of 6 mm were used (as in the past) instead of the newly recommended base thickness of 2.0 mm [3].

III. Calculation of the Antenna Gain in Free Space

The FDTD method may be used to calculate the radiation pattern of the Cisco Model AIR-CB20A-A-K9 PC Card inserted in a laptop computer in free space so that it may be compared with the data available from the manufacturer. Since most of the microwave induced currents for the antenna are for the ground plane immediately underneath the patch antenna, only a limited length of the ground plane beyond the antenna should be enough for proper modeling of the radiated fields. This is verified by calculating the gain of the Model AIR-CB20A-A-K9 PC card antenna for ground plane dimensions of 45.2 × 48 mm (113 × 120 cells) or 45.2 × 60 mm (113 × 150 cells). The calculated gains for the midband irradiation frequency of 5.25 GHz for both cases are identical and 5.8 dBi. The calculated gain is very close to the manufacturer measured gain of 5.6-5.7 dBi for this antenna.

IV. Experimental Measurements of SAR Distribution

As aforementioned, the measurements of the SAR distributions for the Cisco Model AIR-CB20A-A-K9 PC Card inserted into a laptop computer (as in Fig. 1), both for the "above-lap" and "end-on" positions, were done with a planar rectangular box phantom of inside dimensions 12" × 16.5" (30.5 × 41.9 cm) shown in Figs. 4 and 5 for "above-lap" and "end-on" positions, respectively. This box phantom of external dimensions 13" × 17.5" (33 × 44.5 cm) is filled with a

tissue-simulant fluid up to a depth of 15 cm. As recommended in [3], the base thickness of the phantom is 2.0 ± 0.2 mm (0.079"). As seen in Figs. 4 and 5, a 1" thick Styrofoam block is used under the base, except for the region of the wireless laptop to prevent bending of the 2 mm thin base. Also for the SAR testing for the "end-on" position, a separation of 1" (2.5 cm) from the end of the PC card to the bottom of the planar phantom is used.

The tissue-simulant fluid uses a composition developed at the University of Utah which consists of 68.0% water, 31.0% sugar and 1% HEC. For this composition, we have measured the dielectric properties using a Hewlett Packard (HP) Model 85070B Dielectric Probe in conjunction with HP Model 8720C Network Analyzer (50 MHz-20 GHz). The measured dielectric properties at a mid band frequency of 5.30 GHz are as follows: ε_r = 48.5 ± 1.7 and σ = 5.40 ± 0.08 S/m. From the FCC Supplement C [3], we obtain the desired dielectric properties to simulate the body tissue at 5.30 GHz to be ε_r = 48.9 and σ = 5.42 S/m. Thus, the measured properties for the body-simulant fluid are close to the desired values.

V. Calibration of the E-Field Probe

As in some previously reported SAR measurements at 6 GHz [14], we have calibrated the Narda Model 8021 Miniature Broadband Electric Field Probe of tip diameter 4 mm (0.4 to 10 GHz) using a rectangular waveguide WR 159 that was filled with this body-simulant fluid at 5.30 GHz. By comparing the electric fields expected in the tissue from the analytical expressions of the waveguide theory, we obtain a calibration factor of 2.98 (mW/kg)/μV. This is considerably larger than calibration factors of 0.39 and 0.565 (mW/kg)/μV previously reported for the same probe at 835 MHz and 1900 MHz, respectively [15]. This is to be expected since the sensitivity of the diodes used for the Narda Model 8021 Miniature Broadband Electric Field Probe of tip diameter 4 mm is likely to diminish with frequency.

VI. The Measured SAR Distributions

The SAR distributions were determined using the automated SAR measurement system developed at the University of Utah [15]. As described in [15], this SAR measurement system has been validated using a number of wireless telephones at 835 and 1900 MHz, respectively.

The highest SAR region for each of the measurement frequencies (5.18, 5.26, and 5.32 GHz) was identified in the first instance by using a coarser sampling with a step size of 8.0 mm over three overlapping areas for a total scan area of 8.0 × 9.6 cm. After identifying the region of the highest SAR, the SAR distribution was measured with a resolution of 2 mm in order to obtain the peak 1 cm^3 or 1-g SAR. As given in [15], the SAR measurements are performed at 4, 6, 8, 10, 12 mm height from the bottom surface of the body-simulant fluid. The SARs thus measured were extrapolated to obtain values at 1, 3, 5, 7 and 9 mm height and used to obtain 1-g SARs. The uncertainty analysis of the University of Utah SAR measurement system is given in Appendix A. The combined standard uncertainty is ± 8.3%.

The SAR distributions were measured for transmit frequencies of 5.18, 5.26, and 5.32 GHz and are given in Tables 1-3 for the "above-lap" position and in Tables 4-6 for the "end-on" position, respectively. The peak 1-g SARs are summarized in Table 7. For the measurements in Table 1, 2, and 3, the separation between the Cisco Model AIR-CB20A-A-K9 PC Card and the bottom of the experimental phantom is on the order of 1 cm. For the "end-on" position, the separation between the card edge at 90° to the bottom of the flat phantom is 2.5 cm and the SAR distributions at 5.18, 5.26, and 5.32 GHz are given in Tables 4, 5, and 6, respectively.

The experimentally-determined peak 1-g SARs for the "above-lap" position in Tables 1-3 are somewhat lower but of the same order of magnitude as the calculated peak 1-g SAR of 0.146 W/kg in Section II. The slightly lower SARs may well be due to the conducted RF power for this particular laptop being somewhat less than the nominal power of 13.2 dBm assumed for the SAR calculations. In any case, it may be noted that both the calculated and measured 1-g SARs (given in Table 7) are significantly less than the FCC 96-326 guideline of 1.6 W/kg.

VII. Comparison of the Data With FCC 96-326 Guidelines

According to the FCC 96-326 Guideline [1], the peak SAR for any 1-g of tissue should not exceed 1.6 W/kg. For the maximum radiated power condition of 13.2 dBm (20.9 mW), the Cisco AIR-CB20A-A-K9 PC Card has been measured to give peak 1-g SARs of 0.064 to 0.127 W/kg which are considerably smaller than 1.6 W/kg.

REFERENCES

1. Federal Communications Commission, "Guidelines for Evaluating the Environmental Effects of Radiofrequency Radiation," FCC 96-326, August 1, 1996.

2. K. Chan, R. F. Cleveland, Jr., and D. L. Means, "Evaluating Compliance With FCC Guidelines for Human Exposure to Radiofrequency Electromagnetic Fields," Supplement C (Edition 97-01) to OET Bulletin 65, December, 1997. Available from Office of Engineering and Technology, Federal Communications Commission, Washington D.C., 20554.

3. Federal Communications Commission "Supplement C Edition 01-01 to OET Bulletin 65 Edition 97-01" June 2001.

4. K. S. Yee, "Numerical Solution of Initial Boundary Value Problems Involving Maxwell's Equations in Isotropic Media," *IEEE Transactions on Antennas and Propagation,* Vol. AP-14, pp. 302-307, 1966.

5. A. Taflove and M. E. Brodwin, "Computation of the Electromagnetic Fields and Induced Temperature Within a Model of the Microwave Irradiated Human Eye," *IEEE Transactions on Microwave Theory and Techniques,* Vol. MTT-23, pp. 888-896, 1975.

6. A. Taflove, "Application of the Finite-Difference Time-Domain Method to Sinusoidal Steady-State Electromagnetic-Penetration Problems," *IEEE Transactions on Electromagnetic Compatibility*, Vol. EMC-22, pp. 191-202, 1980.

7. K. Umashankar and A. Taflove, "A Novel Method to Analyze Electromagnetic Scattering of Complex Objects," *IEEE Transactions on Electromagnetic Compatibility,* Vol. EMC-24, pp. 397-405, 1982.

8. R. Holland, "THREDE: A Free-Field EMP Coupling and Scattering Code," *IEEE Transactions on Nuclear Science,* Vol. NS-24, pp. 2416-2421, 1977.

9. K. S. Kunz and K. M. Lee, "A Three-Dimensional Finite-Difference Solution of the External Response of an Aircraft to a Complex Transient EM Environment. The Method and Its Implementation," *IEEE Transactions on Electromagnetic Compatibility,* Vol. 20, pp. 328-3342, 1978.

10. O. P. Gandhi, "Some Numerical Methods for EM Dosimetry: ELF to Microwave Frequencies," *Radio Science*, Vol. 30, pp. 161-177, January/February, 1995.

11. O. P. Gandhi, G. Lazzi, and C. M. Furse, "Electromagnetic Absorption in the Human Head and Neck for Mobile Telephones at 835 and 1900 MHz," *IEEE Transactions on Microwave Theory and Techniques*, Vol. 44(10), pp. 1884-1897, 1996.

12. G. Lazzi and O. P. Gandhi, "On the Optimal Design of the PML Absorbing Boundary Condition for the FDTD Code," *IEEE Transactions on Antennas and Propagation,* Vol. 45, pp. 914-916, 1997.

13. ITT Handbook, Reference Data for Radio Engineers, Fifth Edition, Howard W. Sams & Co. Inc, p. 4-19, 1968.

14. O. P. Gandhi and J-Y. Chen, "Electromagnetic Absorption in the Human Head from Experimental 6-GHz Handheld Transceivers," *IEEE Transactions on Electromagnetic Compatibility,* Vol. 39(4), pp. 547-558, 1995.

15. Q. Yu, O. P. Gandhi, M. Aronsson, and D. Wu, "An Automated SAR Measurement System for Compliance Testing of Personal Wireless Devices," *IEEE Transactions on Electromagnetic Compatibility,* Vol. 41(3), pp. 234-245, August 1999.

16. IEEE Std. 1528 - Draft "Recommended Practice for Determining the Peak Spatial-Average Specific Absorption Rate (SAR) in the Human Body Due to Wireless Communication Devices: Experimental Techniques," IEEE SCC34.

Table 1. **Above-lap position.** The SARs measured for the Cisco Model AIR-CB20A-A-K9 PC Card (nominal power of 13.2 dBm) inserted into a laptop computer at 5.18 GHz.

1-g SAR = 0.127 W/kg

a. At depth of 1 mm

0.171	0.184	0.181	0.172	0.164
0.179	0.194	0.189	0.193	0.189
0.188	0.199	0.192	0.187	0.179
0.186	0.187	0.194	0.199	0.193
0.176	0.180	0.202	0.190	0.171

b. At depth of 3 mm

0.140	0.147	0.146	0.139	0.133
0.145	0.156	0.154	0.152	0.149
0.149	0.157	0.153	0.150	0.147
0.149	0.151	0.157	0.159	0.152
0.144	0.148	0.159	0.148	0.135

c. At depth of 5 mm

0.116	0.118	0.119	0.113	0.109
0.119	0.125	0.126	0.121	0.118
0.117	0.124	0.123	0.121	0.121
0.120	0.123	0.127	0.128	0.121
0.117	0.123	0.125	0.116	0.106

d. At depth of 7 mm

0.097	0.097	0.098	0.093	0.090
0.100	0.102	0.104	0.098	0.096
0.096	0.099	0.101	0.099	0.101
0.098	0.102	0.105	0.104	0.096
0.098	0.103	0.100	0.092	0.083

e. At depth of 9 mm

0.084	0.085	0.084	0.080	0.078
0.088	0.086	0.089	0.083	0.082
0.082	0.083	0.086	0.085	0.088
0.085	0.087	0.091	0.088	0.082
0.085	0.090	0.084	0.077	0.068

Table 2. **Above-lap position.** The SARs measured for the Cisco Model AIR-CB20A-A-K9 PC Card (nominal power of 13.2 dBm) inserted into a laptop computer at 5.26 GHz.

1-g SAR = 0.108 W/kg

a. At depth of 1 mm

0.138	0.144	0.154	0.151	0.141
0.141	0.155	0.155	0.150	0.152
0.149	0.161	0.170	0.166	0.156
0.152	0.157	0.164	0.157	0.163
0.142	0.152	0.154	0.155	0.144

b. At depth of 3 mm

0.117	0.120	0.126	0.125	0.117
0.116	0.126	0.126	0.124	0.123
0.124	0.131	0.137	0.135	0.126
0.123	0.128	0.132	0.125	0.127
0.118	0.122	0.124	0.125	0.119

c. At depth of 5 mm

0.101	0.101	0.104	0.104	0.097
0.097	0.104	0.104	0.103	0.100
0.104	0.109	0.112	0.110	0.103
0.102	0.106	0.107	0.100	0.099
0.100	0.100	0.100	0.102	0.098

d. At depth of 7 mm

0.088	0.087	0.088	0.089	0.083
0.083	0.087	0.087	0.088	0.083
0.090	0.091	0.094	0.092	0.086
0.086	0.088	0.088	0.082	0.080
0.085	0.083	0.083	0.085	0.082

e. At depth of 9 mm

0.078	0.078	0.078	0.078	0.073
0.074	0.075	0.077	0.077	0.073
0.080	0.079	0.082	0.079	0.076
0.075	0.076	0.075	0.070	0.069
0.075	0.072	0.072	0.074	0.071

Table 3. **Above-lap position.** The SARs measured for the Cisco Model AIR-CB20A-A-K9 PC Card (nominal power of 13.2 dBm) inserted into a laptop computer at 5.32 GHz.

1-g SAR = 0.096 W/kg

a. At depth of 1 mm

0.122	0.127	0.131	0.129	0.129
0.125	0.131	0.139	0.131	0.125
0.134	0.138	0.129	0.132	0.115
0.114	0.118	0.134	0.123	0.125
0.114	0.116	0.112	0.123	0.119

b. At depth of 3 mm

0.110	0.112	0.112	0.111	0.109
0.108	0.111	0.114	0.113	0.108
0.112	0.113	0.109	0.110	0.100
0.098	0.104	0.110	0.105	0.108
0.101	0.100	0.099	0.104	0.099

c. At depth of 5 mm

0.100	0.099	0.097	0.097	0.094
0.094	0.095	0.095	0.098	0.094
0.095	0.094	0.093	0.093	0.087
0.085	0.091	0.092	0.091	0.094
0.090	0.087	0.088	0.090	0.084

d. At depth of 7 mm

0.091	0.089	0.087	0.087	0.083
0.085	0.083	0.082	0.086	0.085
0.083	0.080	0.082	0.080	0.076
0.076	0.081	0.079	0.081	0.083
0.081	0.077	0.079	0.079	0.074

e. At depth of 9 mm

0.083	0.081	0.080	0.080	0.076
0.079	0.075	0.075	0.078	0.079
0.075	0.071	0.074	0.072	0.068
0.071	0.074	0.072	0.075	0.075
0.075	0.071	0.073	0.072	0.067

Table 4. **End-on position.** The SARs measured for the Cisco Model AIR-CB20A-A-K9 PC Card (nominal power of 13.2 dBm) inserted into a laptop computer at 5.18 GHz. Distance to the bottom of the flat phantom = 2.5 cm.

1-g SAR = 0.089 W/kg

a. At depth of 1 mm

0.137	0.121	0.136	0.140	0.139
0.144	0.141	0.141	0.136	0.137
0.153	0.135	0.132	0.131	0.110
0.130	0.116	0.123	0.115	0.116
0.121	0.115	0.112	0.126	0.086

b. At depth of 3 mm

0.109	0.109	0.110	0.113	0.113
0.120	0.116	0.115	0.114	0.112
0.117	0.110	0.111	0.103	0.091
0.101	0.094	0.097	0.090	0.089
0.093	0.094	0.093	0.097	0.076

c. At depth of 5 mm

0.088	0.097	0.090	0.092	0.093
0.100	0.097	0.095	0.096	0.092
0.091	0.089	0.093	0.080	0.076
0.079	0.076	0.076	0.071	0.068
0.072	0.076	0.078	0.075	0.067

d. At depth of 7 mm

0.072	0.086	0.075	0.077	0.079
0.085	0.082	0.080	0.082	0.078
0.072	0.074	0.078	0.063	0.064
0.062	0.062	0.061	0.057	0.055
0.056	0.063	0.065	0.058	0.058

e. At depth of 9 mm

0.064	0.076	0.066	0.069	0.070
0.074	0.073	0.071	0.072	0.070
0.062	0.063	0.067	0.052	0.055
0.051	0.051	0.050	0.049	0.048
0.047	0.054	0.057	0.047	0.048

Table 5. **End-on position.** The SARs measured for the Cisco Model AIR-CB20A-A-K9 PC Card (nominal power of 13.2 dBm) inserted into a laptop computer at 5.26 GHz. Distance to the bottom of the flat phantom = 2.5 cm.

1-g SAR = 0.082 W/kg

a. At depth of 1 mm

0.113	0.112	0.109	0.122	0.106
0.109	0.107	0.110	0.104	0.108
0.116	0.107	0.113	0.116	0.114
0.119	0.114	0.107	0.120	0.108
0.112	0.125	0.117	0.116	0.108

b. At depth of 3 mm

0.095	0.094	0.093	0.101	0.090
0.091	0.090	0.092	0.088	0.087
0.095	0.090	0.095	0.096	0.094
0.095	0.095	0.092	0.098	0.089
0.093	0.099	0.099	0.096	0.089

c. At depth of 5 mm

0.080	0.080	0.080	0.084	0.077
0.077	0.077	0.077	0.075	0.072
0.078	0.077	0.080	0.079	0.078
0.077	0.079	0.079	0.081	0.073
0.078	0.078	0.082	0.080	0.075

d. At depth of 7 mm

0.069	0.070	0.070	0.071	0.067
0.066	0.067	0.067	0.064	0.061
0.065	0.067	0.069	0.068	0.067
0.064	0.067	0.069	0.069	0.062
0.067	0.064	0.070	0.068	0.063

e. At depth of 9 mm

0.062	0.063	0.064	0.063	0.060
0.057	0.060	0.059	0.056	0.056
0.057	0.060	0.062	0.060	0.061
0.056	0.059	0.062	0.061	0.054
0.060	0.056	0.062	0.060	0.055

Table 6. **End-on position.** The SARs measured for the Cisco Model AIR-CB20A-A-K9 PC Card (nominal power of 13.2 dBm) inserted into a laptop computer at 5.32 GHz. Distance to the bottom of the flat phantom = 2.5 cm.

1-g SAR = 0.064 W/kg

a. At depth of 1 mm

0.072	0.073	0.077	0.064	0.072
0.073	0.075	0.078	0.076	0.074
0.072	0.081	0.077	0.085	0.081
0.079	0.076	0.068	0.0831	0.076
0.081	0.084	0.079	0.062	0.073

b. At depth of 3 mm

0.067	0.068	0.069	0.064	0.067
0.066	0.067	0.069	0.070	0.069
0.066	0.072	0.069	0.073	0.072
0.073	0.069	0.064	0.074	0.071
0.072	0.072	0.070	0.060	0.063

c. At depth of 5 mm

0.062	0.064	0.063	0.063	0.062
0.061	0.061	0.062	0.065	0.064
0.062	0.064	0.063	0.064	0.064
0.067	0.063	0.060	0.066	0.066
0.064	0.063	0.062	0.057	0.055

d. At depth of 7 mm

0.059	0.060	0.058	0.061	0.058
0.057	0.057	0.057	0.062	0.060
0.059	0.059	0.059	0.058	0.059
0.063	0.059	0.058	0.061	0.062
0.059	0.058	0.056	0.054	0.049

e. At depth of 9 mm

0.056	0.057	0.054	0.058	0.055
0.054	0.054	0.054	0.059	0.057
0.057	0.057	0.055	0.055	0.056
0.059	0.056	0.055	0.058	0.059
0.056	0.055	0.051	0.050	0.045

Table 7. The peak 1-g SARs measured for the Cisco Model AIR-CB20A-A-K9 PC Card (nominal power of 13.2 dBm) inserted into a laptop computer.

		1-g SAR in W/kg		
PC position relative to the flat phantom	Spacing to the bottom of the phantom	5.18 GHz	5.26 GHz	5.32 GHz
"Above-lap": bottom of PC pressed against bottom of the flat phantom	1 cm	0.127	0.108	0.096
"End-on": card edge at 90° relative to the bottom of the flat phantom	2.5 cm	0.089	0.082	0.064

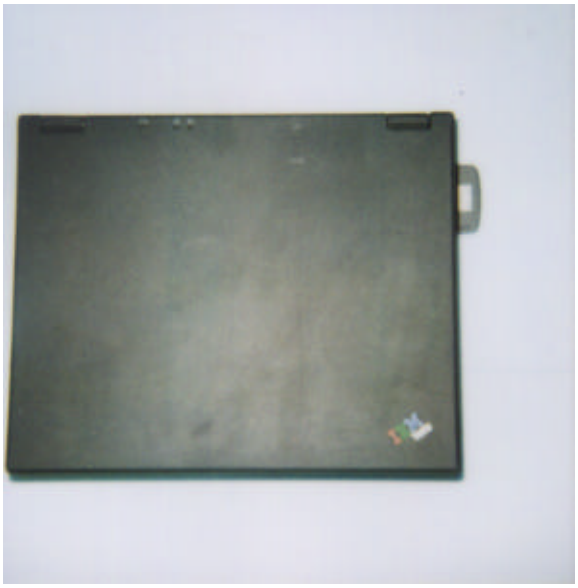

Fig. 1. Photograph of the Cisco Model AIR-CB20A-A-K9 PC Card inserted into a laptop computer.

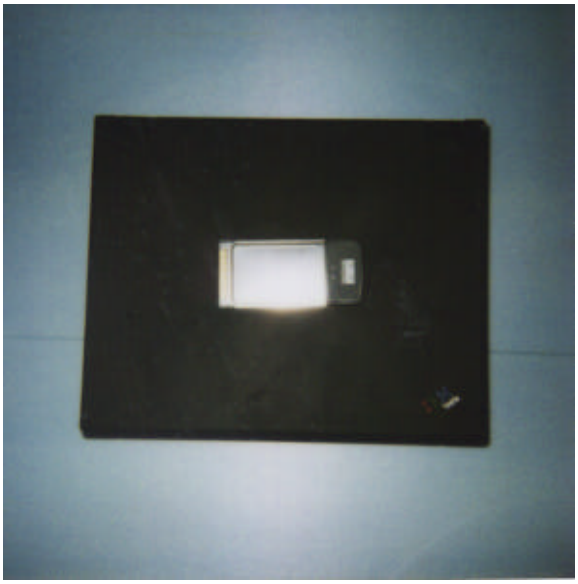

Fig. 2. A picture of the Model AIR-CB20A-A-K9 PC Card placed on the laptop computer.

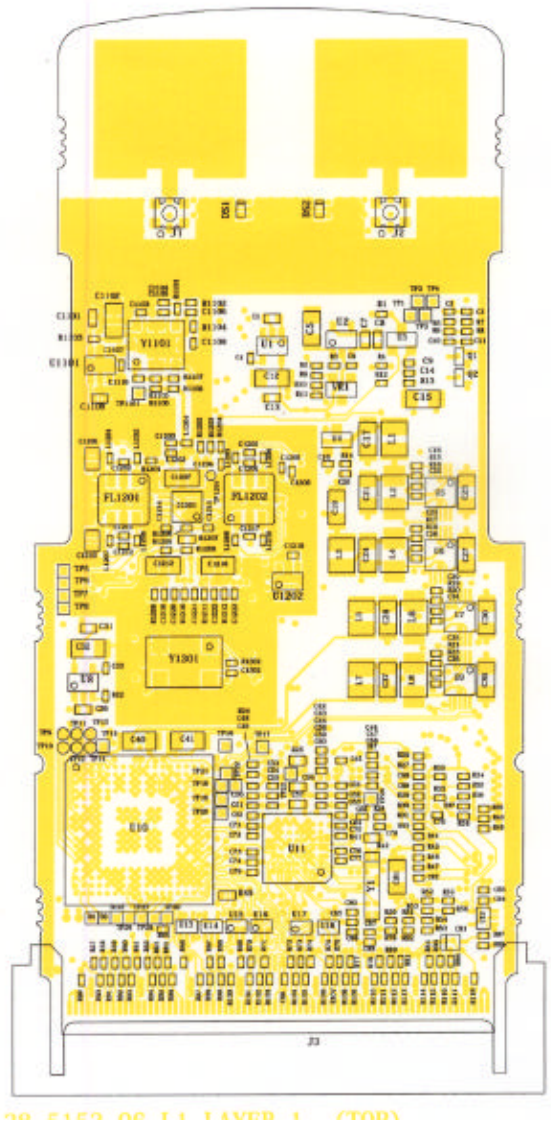

a. Top view showing the two patch antennas.

Fig. 3. Some engineering drawings for the antenna layout on PCB for Cisco Model AIR-CB20A-A-K9 PC Card.

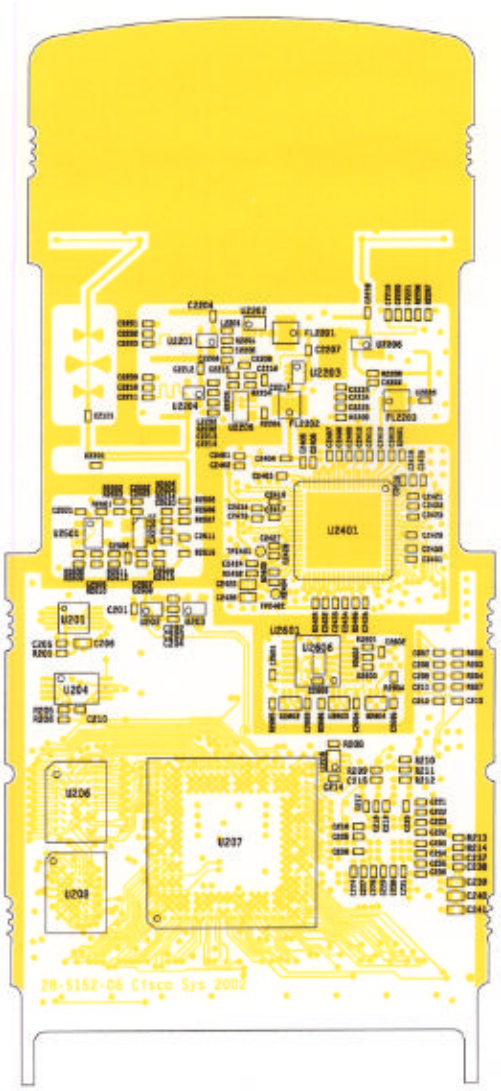

b. Back view showing the ground plane for the two patch antennas.

Fig. 3. Some engineering drawings for the antenna layout on PCB for Cisco Model AIR-CB20A-A-K9 PC Card.

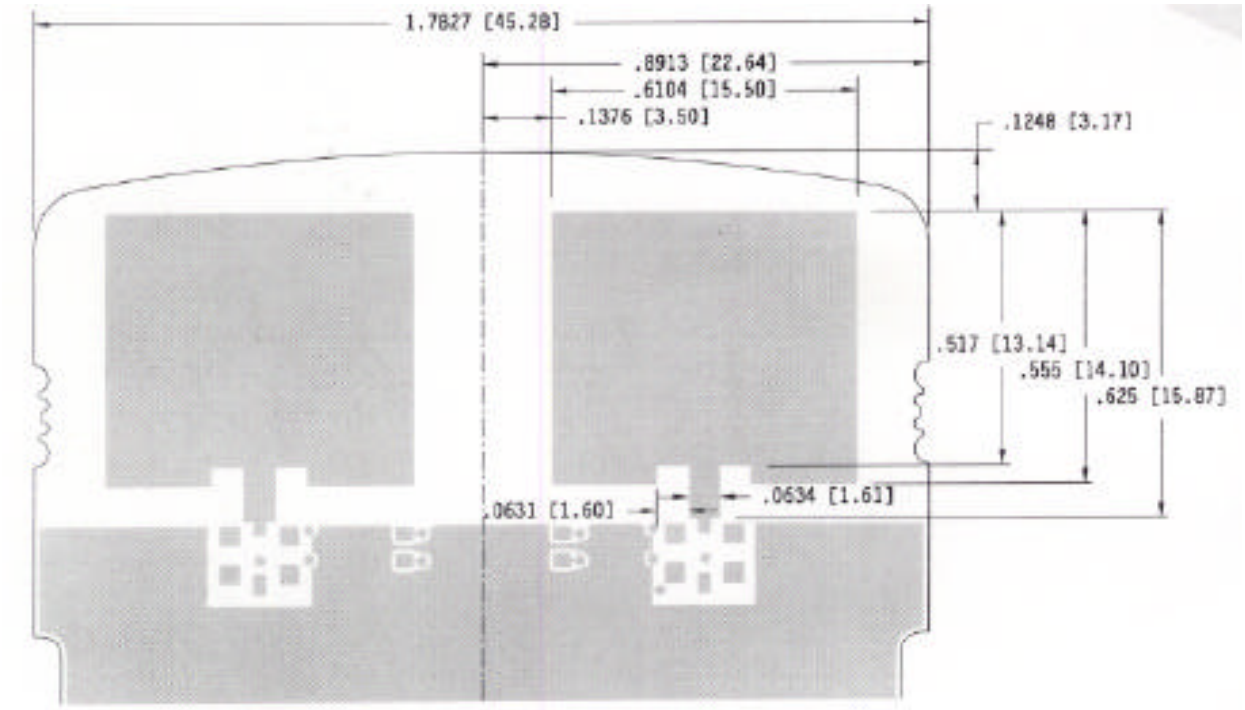

c. A detailed drawing of the dimensions of the patch antennas in inches and (mm within parentheses.

Fig. 3. Some engineering drawings for the antenna layout on PCB for Cisco Model AIR-CB20A-A-K9 PC Card.

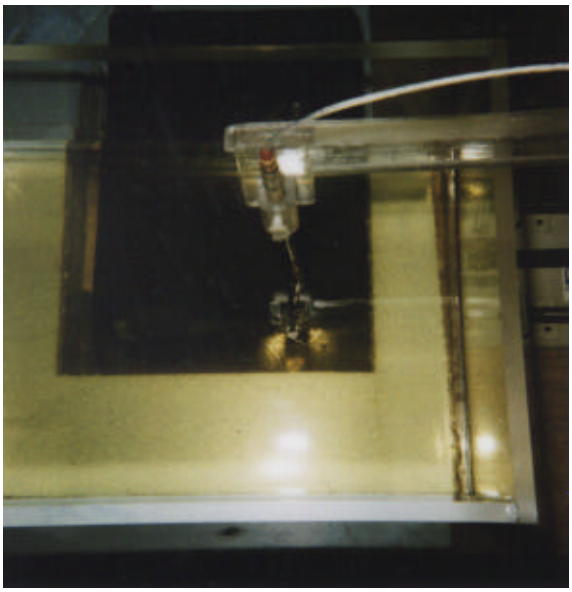

Fig. 4. Photograph of the Cisco Model AIR-CB20A-A-K9 PC Card inserted into a portable computer (as in Fig. 1) placed with the bottom pressed against the base of the planar tissue-simulant phantom. A Styrofoam block is used under the base to prevent bending of the 2 mm thin base of the phantom.

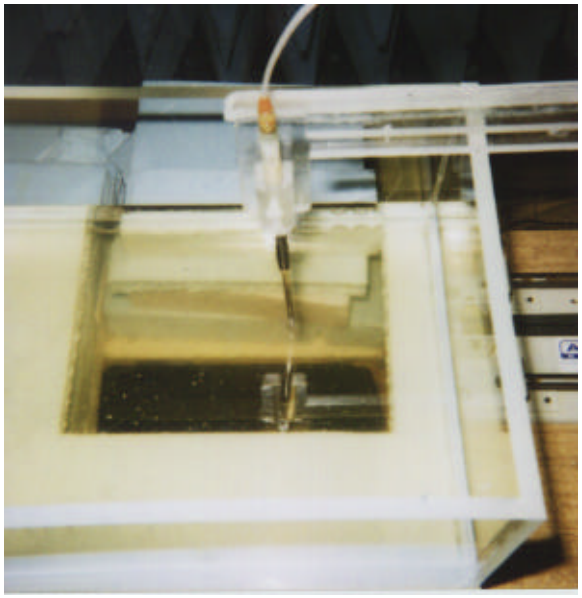

Fig. 5. Photograph of the Cisco Model AIR-CB20A-A-K9 PC Card inserted into a portable computer (as in Fig. 1) placed with the card edge at 90° and separated from the bottom of the phantom by 2.5 cm for "end-on" testing of SAR. As in Fig. 4, here too, a Styrofoam block is used under the base to prevent bending of the 2 mm thin base of the phantom.

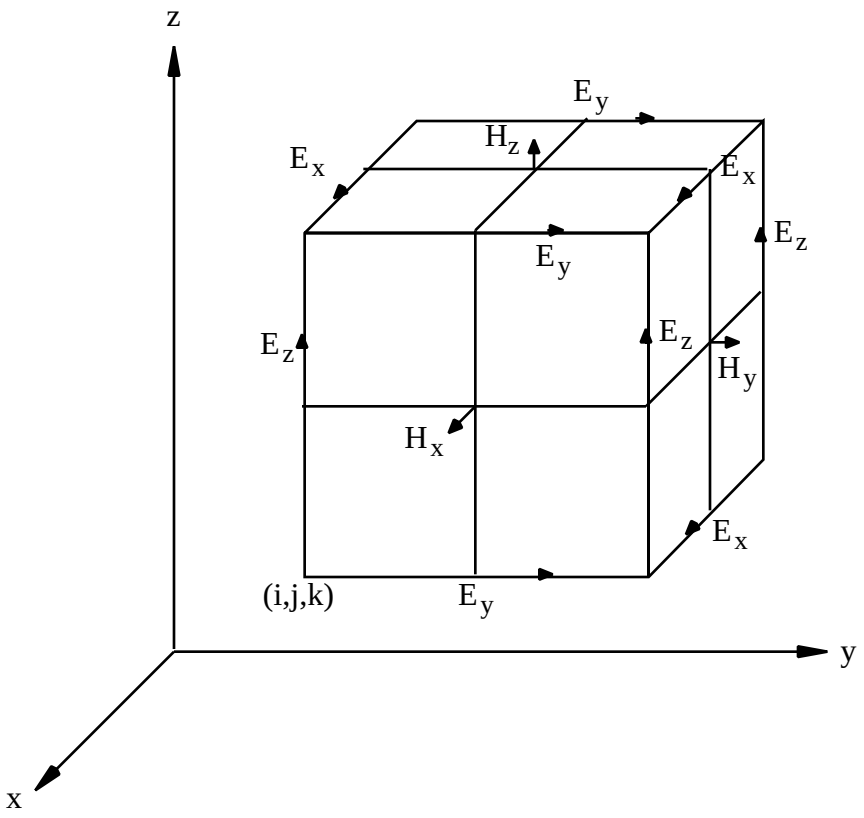

Fig. 6. A unit cell of Yee lattice indicating positions for the various field components.

APPENDIX A

Uncertainty Analysis

The uncertainty analysis of the University of Utah SAR Measurement System is given in Table A.1. Several of the numbers on tolerances are obtained by following procedures similar to those detailed in [15], while others have been obtained using methods suggested in [16].

Table A.1. Uncertainty analysis of the University of Utah SAR Measurement System.

Uncertainty Component	Tolerance ± %	Prob. Dist.	Div.	C_i 1-g	1-g u_i ± %
Measurement System					
Probe calibration	2.0	N	1	1	2.0
Axial istropy	4.0	R	√3	$(1\text{-cp})^{1/2}$	1.6
Hemispherical isotropy	5.5	R	√3	$\sqrt{c_p}$	0.0
Boundary effect	0.8	R	√3	1	0.5
Linearity	3.0	R	√3	1	1.7
System detection limits	1.0	R	√3	1	0.6
Readout electronics	1.0	N	1	1	1.0
Response time	0.0	R	√3	1	0.0
Integration time	0.5	R	√3	1	0.3
RF ambient conditions	0	R	√3	1	0
Probe positioner mechanical tolerance	0.5	R	√3	1	0.3
Probe positioning with respect to phantom shell	2.0	R	√3	1	1.2
Extrapolation, interpolation, and integration algorithms for max. SAR evaluation	5.0	R	√3	1	2.9
Test Sample Related					
Test sample positioning	3	R	√3	1	1.7
Device holder uncertainty	3	R	√3	1	1.7
Output power variation - SAR drift measurement	5	R	√3	1	2.9
Phantom and Tissue Parameters					
Phantom uncertainty - shell thickness tolerance	10.0	R	√3	1	5.8
Liquid conductivity - deviation from target values	0.4	R	√3	0.7	0.2
Liquid conductivity - measurement uncertainty	1.5	R	√3	0.7	0.6
Liquid permitivity - deviation from target values	0.8	R	√3	0.6	0.3
Liquid permittivity - measurement uncertainty	3.5	R	√3	0.6	1.2
Combined Standard Uncertainty		RSS			8.3
Expanded Uncertainty (95% Confidence Level)					16.6